Cellular Physiology and Biochemistry

Cell Physiol Biochem 2018;51:1645-1657
DOI: 10.1159/000495652
Published online: 29 November, 2018
Accepted: 21 November 2018

Original Paper

Involvement of the TLR4/NF-κB Signaling Pathway in the Repair of Esophageal Mucosa Injury in Rats with Gastroesophageal Reflux Disease

Hai-Xiang Yu Xiao-Long Wang Le-Ning Zhang Ji Zhang Wei Zhao

Department of Thoracic Surgery, China-Japan Union Hospital of Jilin University, Changchun, China

Key Words
TLR4/NF-κB signaling pathway • Gastroesophageal reflux disease • Esophageal mucosal injury • Lipopolysaccharide • Repair • Rat models

Abstract
Background/Aims: Numerous studies have highlighted the activation of NF-κB in the esophageal mucosa during the early stages of gastroesophageal reflux disease (GERD). The present study aimed to investigate the role of the TLR4/NF-κB signaling pathway in GERD rat models. ***Methods:*** Wistar rats (n = 60) were recruited to establish a GERD animal model. Distal esophageal pH was assessed, followed by determination of the contents of thiobarbituric acid-reactive species (TBARS) and reactive oxygen species (ROS) in esophageal mucosa homogenate. ELISA was employed to detect the levels of inflammatory factors (IL-6, IL-8, IL-10 and TNF-α) in esophageal mucosa. The expression of MMP-3, MPP-9, Cldn1 and Cldn4 was determined by immunohistochemistry. RT-qPCR and western blot analysis were applied to evaluate the protein expressions in TLR4/NF-κB signaling pathway, while TUNEL staining was utilized to examine the apoptosis rate in the esophageal mucosal tissues. ***Results:*** Distal esophageal pH of the rats was higher in the GERD + PDTC group than in other groups. Levels of inflammatory factors in esophageal mucosal tissues were downregulated with the inhibition of NF-κB, which was determined to be associated with the decreased contents of TBARS and ROS. Moreover, decreased MMP-3 and MPP-9 in addition to elevated Cldn1 and Cldn4 were detected in the esophageal mucosa as a result of the inactivation of NF-κB. The TLR4/NF-κB signaling pathway-related proteins (TLR4, NF-κB and IκBα); the rate of apoptosis was demonstrated to be suppressed in the GERD + PDTC group, while inactivating NF-κB was found to alleviate the tissue damage observed in the esophageal mucosa. ***Conclusion:*** The key findings of the current study demonstrate that the inactivation of the TLR4/NF-κB signaling pathway alleviates oxidative stress injury and promotes the repair of esophageal mucosal injury among rats with GERD, highlighting a potential novel GERD mechanism.

Dr. Wei Zhao

Department of Thoracic Surgery, China-Japan Union Hospital of Jilin University
No. 126, Xiantai Street, Changchun 130033, Jilin Province (China)
Tel. +86-0431-84997545, E-Mail zhaowei_drz@163.com

Introduction

Gastroesophageal reflux disease (GERD) represents a common disorder of the gastrointestinal tract characterized by the backflow of gastric contents in the upper digestive tract [1]. The major ubiquitous signs of GERD include heartburn and acid regurgitation, while other commonly reported symptoms include sore throat, nausea, eructation, chest pain and cough [2]. Among European and American populations, the approximate prevalence rate of GERD has been reported to be between 10%–20%, while in Asia, this number is below 10% [3, 4]. Possible risk factors associated with the condition include age, obesity, alcohol consumption, cigarette smoking and presence of hiatus hernia [5]. Mahadeva et al. concluded that GERD is more common among persons of British origin compared to people of the South-East Asian dyspeptic population, suggesting that race and/or western lifestyle are crucial contributors to the occurrence of GERD [6]. Esophageal injuries are the most overt complications associated with GERD, including erosive esophagitis, Barrett's esophagus, and esophageal stricture [4]. The physiological mechanism by which normal esophageal mucosa involves the maintenance of an effective barrier restraining acidic refluxate within the esophageal lumen [7]. Hence, the restoration of esophageal mucosa integrity represents an efficient and innocuous approach by which GERD could be alleviated. Accumulating studies exploring potential therapeutic targets have highlighted berberine and esophageal mucosal damage in reflux esophagitis caused by suppressing proinflammatory cytokines and cyclooxygenase-2, as well as reflux-related esophageal histological changes and the therapeutic use of melatonin in GERD [8-10].

As a widely expressed transcription factor, nuclear factor-kappa B (NF-κB) regulates various genes that encode inflammatory mediators and serves as a crucial downstream target of mitogen-activated protein kinase (MAPK) signaling pathways in inflammatory and immune responses [11]. Toll-like receptors (TLRs) are transmembrane proteins that are primarily tasked with the recognition of pathogen-associated molecular patterns that are present on viral and bacterial products, among which Toll-like receptor 4 (TLR4) triggers the activation of NF-κB by recruiting myeloid differentiation factor 88 (Myd88) [12]. TLR4/NF-κB signaling, a classical signaling pathway, is involved in the regulation as well as the inflammatory response of cell proliferation and apoptosis [11]. A previous study concluded that adoptive regulatory T-cell therapy attenuated subarachnoid hemorrhage-induced cerebral inflammation by suppressing the TLR4/NF-κB signaling pathway [13]. Another study revealed that andrographolide could possess anti-cancer properties capable of modulating the TLR4/NF-κB signaling pathway in insulinoma [14]. The inflammatory response might be alleviated by single immunoglobulin IL-1-related receptor via blockade of the TLR4/NF-κB signaling pathway [15]. Despite the fact that the TLR4/NF-κB pathway has been extensively reviewed, studies investigating its potential effect on GERD, particularly on esophageal mucosal injury, are rare. Therefore, the central objective of the current study was to explore the mechanism by which the TLR4/NF-κB signaling pathway influences esophageal mucosal injury in a GERD rat model.

Materials and Methods

Animals

A total of sixty 8-week-old male Wistar rats (weighing 256-343 g) were recruited from the Beijing Vital River Laboratory Animal Technology Co., Ltd. (Beijing, China) and housed under specific controlled conditions: a 12-h light/dark cycle, 25°C, free access to water and food one week prior to either surgery or the sham operation. All experiments were conducted under the approval of the Ethics Committee of the China-Japan Union Hospital of Jilin University for the use of animals and performed in strict accordance with relevant regulations set by the International Association for the Study of Pain for the protection and use of laboratory animals.

Animal grouping and model establishment

GERD rat models were established [16]. The rats were deprived of food for 24 h prior to the operative procedure and intraperitoneally anesthetized with 1% sodium pentobarbital. Abdominal hair removal was followed by disinfection with 75% alcohol. A 3-cm subxiphoid incision was made along the ventral midline, and the abdominal cavity was then opened to fully expose the abdominal portion of the esophagus and stomach. The anterior wall of the cardia was incised vertically along the midline to expose the esophageal-gastric junction. The incision was 1.2 cm, 2/3 on the upper part of the junction and 1/3 on the lower part. Incisions were closed in a transverse manner with 6-0 non-absorbable nylon sutures. A gastric tube was promptly inserted into the incision, followed by the administration of 2 mL of normal saline solution, after which the tube was removed and one side of the esophagus was closed with tweezers. Gastric fluid was squeezed from the other side toward the closed side to confirm whether the sutures were leaking. Ten milliliters of normal saline solution was then injected into the abdominal cavity to compensate for the body fluid lost during the operation. The muscle layer of the abdominal wall was subsequently closed with continuous 4-0 non-absorbable nylon sutures, and the skin was finally closed with interrupted sutures. The abdominal cavity was closed.

The sham-operated rats were subjected to the following. Pre- and post-operation diet management and anesthesia were identical to the model group. The ligament of the gastric fundus was dissociated but not ligated after the abdominal cavity had been opened. The abdominal portion of the esophagus and the stomach was fully exposed, with the former dissociated and the anterior wall of the cardia kept intact. A gastric tube was inserted into the incision after 20 min and 2 mL of normal saline solution was injected. After the tube had been removed, 10 mL of normal saline solution was again injected into the abdominal cavity, and the cavity was then closed. After the operation, the animals were housed in single cages, placed on a fasting diet for 48 h and granted free access to water. During the fast, rats received subcutaneous injection of 5 mL of glucose saline solution. The rats were then granted free access to water and food. Activity, water intake, feces and weight changes were recorded.

After model establishment was confirmed, the GERD rats were randomly assigned into 3 groups with 12 rats in each group: GERD group, GERD + PDTC group (PDTC: pyrrolidine dithiocarbamate, a specific inhibitor of NF-κB) and GERD + LPS group (LPS: lipopolysaccharide, a specific activator of NF-κB). Normal group and sham operation (sham) group were set up with the same number of rats. Rats in the GERD + PDTC group and GERD + LPS group received intraperitoneal injection of 100 mg/kg PDTC (Gochembio Inc., Wuxi, China) and LPS (Beyotime Biotechnology Inc., Shanghai, China) at a concentration of 2% 60 min after model establishment. The rats in the other three groups received an intraperitoneal injection of phosphate-buffered saline (PBS) at an equal volume. Intraperitoneal injections were continually administered to rats in all groups for 27 consecutive days.

Esophageal pH testing

On the 28th day post-operation, esophageal pH was examined using Digitrapper MKIII (Synectics Medical, Stockholm, Sweden). The rats were positioned on the operation table after intraperitoneal anesthesia. The pH detector tube was inserted into the distal esophagus via the mouth, 8 cm from the incisor, with the values then recorded accordingly.

Hematoxylin-eosin (HE) staining

After 28 days of model establishment, the esophagus was removed and washed. Esophageal mucosa (0.5 cm^3) was cut and fixed in 10% formaldehyde solution (163101, Beijing Solarbio Science & Technology Co., Ltd., Beijing, China) for 12-24 h as the sample. The sample was dehydrated, cleared, immersed, paraffin embedded and constructed into 5 μm serial sections. The sections were then deparaffinized in xylene, washed with 85%, 90% and 95% ethyl alcohol respectively, rinsed in water, stained in 1% hematoxylin for 5 min, rinsed in water, and destained in 1% diluted hydrochloric acid alcohol for 15 s and again rinsed in water. The sections were then shifted to blue using 0.1% ammonia for 30 s, stained in 0.5% eosin for 30 s, dehydrated with alcohol, fixed with xylene, and mounted in neutral balsam. Pathomorphological characteristics were observed and evaluated using an optical microscope.

Masson staining

The sections were fixed, rinsed under running tap water and stained using Mayer's hematoxylin for 5 min. The sections were then differentiated in 1% acid alcohol, rinsed under running tap water, stained in Ponceau S acid solution for 5-10 min and washed in distilled water. After that, they were again differentiated in 1% phosphomolybdic acid aqueous solution for 5 min, transferred directly to aniline blue or bright green solution to stain for 5 min and differentiated in 1% glacial acetic acid solution for 5 min. The sections were then subjected to a repeated dehydration procedure with alcohol, cleared in xylene and finally mounted with neutral balsam. After staining, collagen appeared blue, cytoplasm, muscle fiber and red blood cells appeared red, and the nucleus appeared dark blue.

Enzyme-linked immunosorbent assay (ELISA)

On the 28th day after model establishment, rats in all groups were anesthetized. A 1.5-2.0 cm long esophagus was removed to make into 10% esophageal homogenate. An ELISA Kit (96T, Shanghai Meilian Biotechnology, Co., Ltd., Shanghai, China) was used according to the manufacturer's instructions, and the optical density (OD) of each well was measured at a wavelength of 450 nm absorption with a universal enzyme marker (Model: RT-2100C, Rayto Life and Analytical Sciences Co., Ltd., Shenzhen, China). A standard curve was drawn, and the levels of interleukin (IL)-6, IL-8, IL-10 and tumor necrosis factor (TNF)-α in the esophageal mucosa of rats was quantified and subsequently analyzed. The test was repeated three times.

Determination of oxidative stress (OS) indicators

Lower esophageal (including the anastomotic stoma) was incised longitudinally and cleaned using 0.9% sodium chloride solution. Following the addition of 500 μL normal saline at 4°C, 0.5-1% tissue homogenate was prepared based on the ratio of weight and volume in an ice-bath using the homogenizer and centrifuged at 1610 × g at low temperature for 10 min, with the supernatant obtained and preserved at -80°C. Thiobarbituric acid-reactive species (TBARS) chromometry was employed to measure the content of TBARS in homogenate. The reactive oxygen species (ROS) content in homogenate was determined using ELISA. The well plate was added with 190 μL homogenate supernatant and 10 μL dichlorofluorescin diacetate (DCFH-DA) with the concentration of 1 mmol/L and then placed in the microplate reader to detect the ROS content for analysis. The experiment was repeated three times.

Immunohistochemistry

On the 28th day after model establishment, paraffin sections of esophageal mucosa tissue with a thickness of 3 μm were prepared. The sections were deparaffinized using conventional xylene, dehydrated with gradient alcohol, and washed three times with PBS (0.01 M, pH = 7.4) 3 min per wash. After antigen retrieval using citric acid repair liquid at 98°C for 5 min, each section was incubated with a drop of streptavidin-peroxidase (SP) liquid at room temperature for 10 min and washed an additional 3 times with PBS (3 min each). Following the addition of 10% normal goat serum blocking solution, each section was then incubated in the wet box overnight at 4°C with monoclonal rabbit antibody matrix metalloproteinase-3 (MMP-3) (1:100, ab52915), matrix metalloproteinase-9 (MMP-9) (1:1000, ab38898), claudin-1 (Cldn1) (1:200, ab15098), and claudin-4 (Cldn4) (1:200, ab217685). All the above mentioned antibodies were purchased from Abcam Inc. (Cambridge, MA, USA). Each section was then incubated with the secondary antibody, biotinylated goat anti-rabbit immunoglobulin G (IgG) (1:200, ab6721, Abcam Inc., Cambridge, MA, USA), at 37°C for 1 h and the SP compound diluted 100 times (E030100, Beijing Hong Yue Creative Technology Co., Ltd., Beijing, China) at 37°C for 1 h. The sections were developed using diaminobenzidine (DAB) reagent for 10 min. Negative cells displayed no coloration, weakly positive cells were light yellow, moderately positive cells were brown yellow, and strongly positive cells were brown. The sections were positive in the event the number of positive cells was > 10%. Five different visual fields were selected from each section under the guidance of an inverted microscope (XDS-800D, Shanghai Caikon Optical Instrument Co. Ltd., Shanghai, China) for image acquisition. The ratio of positive cells to total cells among the visual fields was determined; the positive expression rate = number of positive cells/number of total cells.

Reverse transcription quantitative polymerase chain reaction (RT-qPCR)

Total RNA was extracted using a reagent kit (QIAGEN, Valencia, CA, USA) in accordance with the instructions. The complementary DNA (cDNA) was synthesized from the isolated RNA using a reagent kit (QIAGEN, Valencia, CA, USA). The PCR primers (Table 1) were designed using the Primer 5.0 software based on the gene sequence published in the GenBank database and then synthesized (Sangon Biotech Co., Ltd, Shanghai, China). The volume of each PCR mix was 20 μL, including SYBR PremixExTaq 10 μL, Forward Primer 0.8 μL, Reverse Primer 0.8 μL, ROX Reference Dye II 0.4 μL, template DNA 2 μL and dH_2O 6.0 μL. qPCR was performed with an initial pre-denaturation at 95°C for 30 s, followed by denaturation at 95°C for 5 s, annealing at 60°C for 30 s, and extension at 72°C for 30 s (40 cycles altogether). β-actin was regarded as the internal control. Each gene in the samples was measured in triplicate. The reliability of the PCR results was verified in correspondence with the dissolution curve. The cycle threshold (Ct, which is the inflection point on the amplification power curve) was calculated, and the relative gene expression was calculated using the $2^{-\Delta\Delta Ct}$ method ($\Delta Ct = Ct_{(target\ gene)} - Ct_{\beta\text{-actin}}$, $\Delta\Delta Ct = \Delta Ct_{(target\ gene)} - \Delta Ct_{\beta\text{-actin}}$).

Table 1. Primer sequences for RT-qPCR. Notes: TLR4, Toll-like receptor 4; NF-κB, nuclear factor-kappa B; RT-qPCR, reverse transcription quantitative polymerase chain reaction

Gene	Direction	Primer sequence (5' - 3')
TLR4	Forward	CTCACAACTTCAGTGGCTGGATTTA
	Reverse	GTCTCCACAGCCACCAGATTCTC
NF-κB	Forward	CATGCGTTTCCGTTACAAGTG
	Reverse	GTGCGTCTTAGTGGTATCTGTGCT
IκBα	Forward	TGACCATGGAAGTGATTGGTCAG
	Reverse	GATCACAGCCAAGTGGAGTGGA
β-actin	Forward	GGAGATTACTGCCCTGGCTCCTA
	Reverse	GACTCATCGTACTCCTGCTTGCTG

Western blot analysis

On the 28th day after model establishment, rat esophageal mucosal tissues of each group were cut into pieces, added into tissue lysate, cracked on ice and centrifuged. The protein concentrations of the extracted supernatant liquid were measured using a BCA Kit (Beyotime Biotechnology, Shanghai, China). The extracted proteins were mixed with 5 × loading buffer and boiled for 5 min at 100°C. The samples were then subjected to sodium dodecyl sulfate-polyacrylamide gel electrophoresis (SDS-PAGE). Separated proteins on the gel were subsequently transferred onto a polyvinylidene fluoride (PVDF) membrane at 4°C for 2 h (constant current, 65 V). Membrane blockade was performed using 5% fat-free dry milk for 1 h at room temperature and washed in phosphate buffer solution with Tween 20 (PBST). The membrane was subsequently incubated with primary antibodies overnight at 4°C, including rabbit anti-human TLR4 polyclonal antibody (dilution, 1:500; ab13556), rabbit anti-human NF-κB polyclonal antibody (dilution, 1:1000; ab32360), rabbit anti-IκBα (dilution, 1:1000; ab109300) and anti-β-actin polyclonal antibody (dilution, 1:500; ab8226). The membrane was then washed in PBST and incubated with horseradish peroxidase-conjugated rabbit anti-mouse IgG (dilution, 1:3000; ab6785) secondary antibody for 60 min at room temperature. After three PBST washes, the membrane was exposed to X-ray film, which was then developed and fixed. Optical densities were obtained using Bio-Rad Quantity 4.5.2 software, from which the protein expression levels were calculated. The experiment was performed three times. All antibodies used in the assay were purchased from Abcam Inc. (Cambridge, MA, USA).

Terminal dUTP nick-end labeling (TUNEL) assay

The paraffin-embedded tissue samples were sectioned at 5-μm thickness, deparaffinized and dehydrated and incubated for 15 min at room temperature. Cell apoptosis was evaluated using an *in situ* cell death detection kit (11684817910; Shanghai Ebioeasy Co., Ltd., Shanghai, China) based on its protocol. The samples were then rinsed with PBS, incubated in 50 μL TUNEL reaction mixture for 1 h at 37°C in a humidified chamber, rinsed 2-3 times in PBS and dried. Then, they were incubated in 50 μL transforming agent peroxidase for 30 min at 37°C in a humidified chamber and rinsed 3 times with PBS. The sections were then finally incubated in 50-100 μL diaminobenzidine for 10 min at room temperature and rinsed three times with PBS. The nucleus was counterstained with hematoxylin and mounted. Cells observed to be pale brown or dark brown under optical microscope were considered positive. Apoptosis rate was calculated by tallying the total apoptotic cells in 5 microscopic fields of each sample (six samples from each group).

Statistical analysis

All data were analyzed using the SPSS 21.0 statistical software (IBM Corp. Armonk, NY USA). The measurement data are presented as the mean ± standard deviation (SD). The comparisons among multiple groups were conducted using one-factor analysis of variance (ANOVA). Differences between experimental groups were determined by Fisher's least significant difference (LSD) post-test. Expression of MMP-3, MPP-9, Cldn1, and Cldn4 was compared between groups using the rank-sum test. A probability value of $P < 0.05$ was considered statistically significant.

Results

Inactivated NF-κB increases distal esophageal pH

Initially, the distal esophageal pH of each group was measured. On the 28th day after model establishment, distal esophageal pH in the sham group and GERD + PDTC group was relatively stable compared with the normal group ($P_{\text{Normal VS Sham}} = 0.861$, $P_{\text{Normal VS GERD+PDTC}} = 0.605$, $P_{\text{Sham VS GERD+PDTC}} = 0.991$). The pH values in the GERD group and GERD + LPS group were reduced compared with the normal group and the sham group (both $P < 0.0001$). Compared with the GERD group, the pH values in the GERD + PDTC group increased significantly ($P < 0.0001$), while that in the GERD + LPS group was remarkably reduced ($P_{\text{GERD VS GERD+LPS}} = 0.020$) (Fig. 1), indicating that decreased NF-κB increases distal esophageal pH.

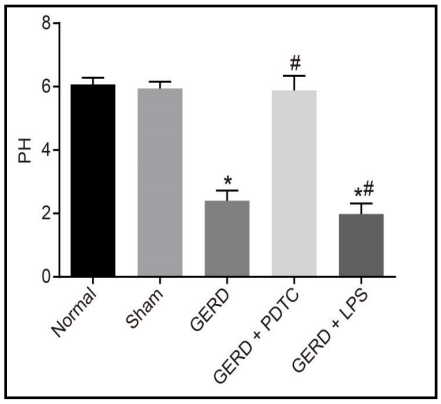

Fig. 1. Distal esophageal pH of the five groups on the 28th day after model establishment. *, P<0.05 vs. the normal group and the sham group; #, P<0.05 vs. the GERD group; GERD, gastroesophageal reflux disease; PDTC, pyrrolidine dithiocarbamate; LPS, lipopolysaccharide.

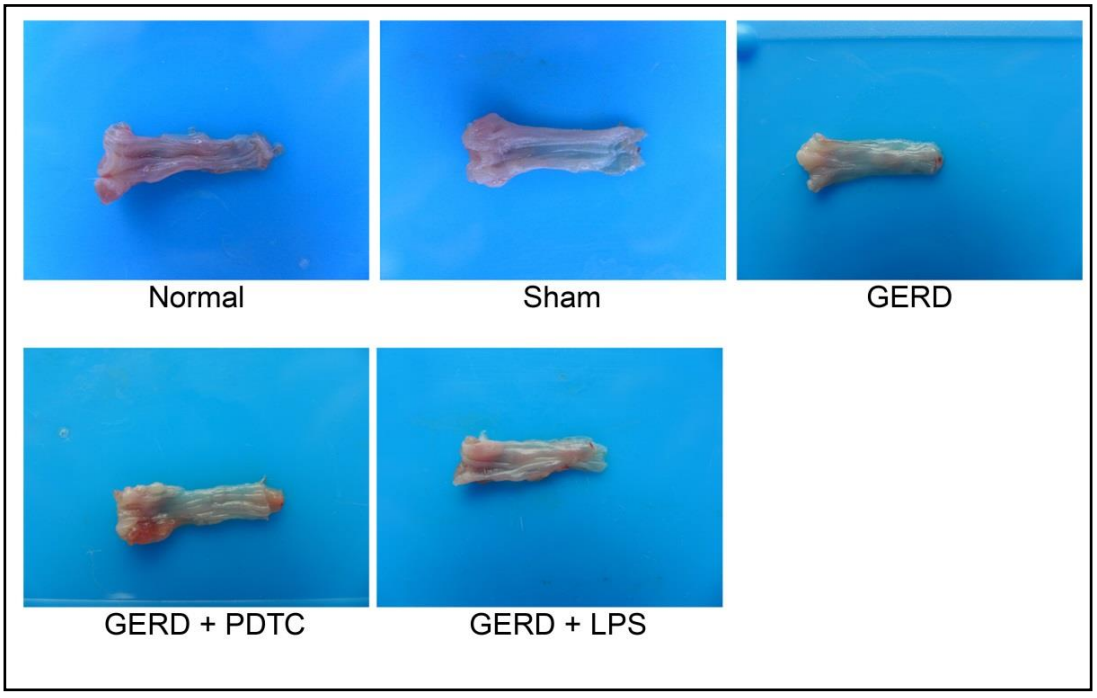

Fig. 2. General condition of esophageal mucosa of rats in the five groups. GERD, gastroesophageal reflux disease; PDTC, pyrrolidine dithiocarbamate; LPS, lipopolysaccharide.

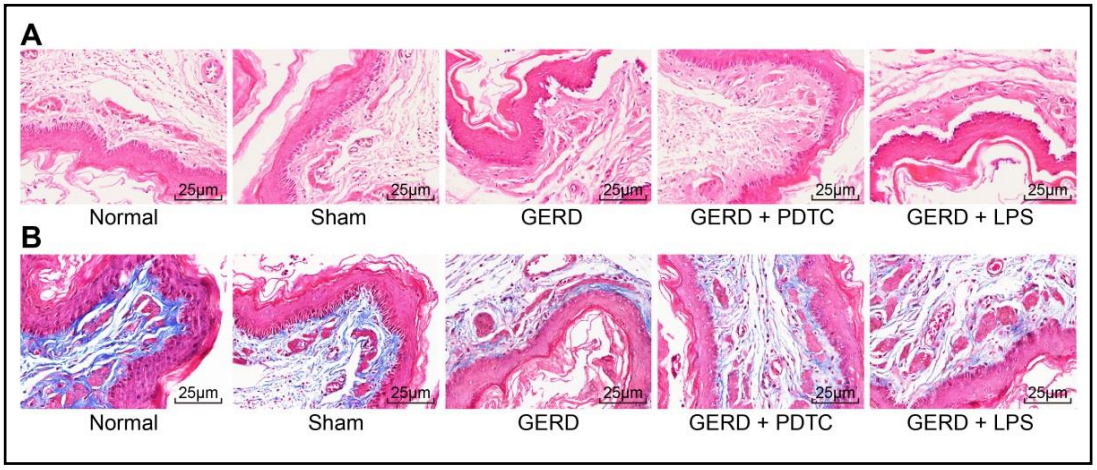

Fig. 3. Pathological changes to esophageal mucosa observed after HE staining (100 ×) and Masson staining (400 ×). GERD, gastroesophageal reflux disease; PDTC, pyrrolidine dithiocarbamate; LPS, lipopolysaccharide; HE, hematoxylin-eosin.

Inactivated NF-κB alleviates tissue damage of esophageal mucosa

The esophageal samples were analyzed to explore the effect of the TLR4/NF-κB signaling pathway on tissue damage of esophageal mucosa. As shown in Fig. 2, the mucosal integrity and smoothness underwent no evident changes among the rats in the sham group and normal group. Hyperemia at varying degrees, erosions, leukoplakia, esophageal wall thickening and irregular esophageal thickening were observed in esophageal mucosal tissues in the GERD group and GERD + LPS group. The esophageal mucosal injuries were well-healed in the GERD + PDTC group. The above results demonstrated that tissue damage of the esophageal mucosa is alleviated after NF-κB is inhibited.

Decreased NF-κB inhibits inflammatory response

To investigate the means by which the TLR4/NF-κB signaling pathway affects the inflammatory response, HE staining and Masson staining were performed to evaluate the pathological changes to esophageal mucosae. No inflammatory changes were observed in esophageal mucosae in the normal group, sham group or GERD + PDTC group. Esophageal mucosal sections of the GERD group and GERD + LPS group showed different degrees of inflammatory changes (reflux esophagitis), squamous epithelial hyperplasia, papilla extension in the mucosal lamina propria, inflammatory cell infiltration and erosion, and ulcer (Fig. 3A). Discrete collagen fibrils were detected in the lamina propria of rats in the normal group and sham group. In the GERD group and GERD + LPS group, exudates, inflammatory cell infiltration and a great number of collagen fibrils among inflammatory cells were also detected. In the GERD + PDTC group, mature granulation tissues were found in the lamina propria of the esophageal epithelium, and collagen fibrils increased slightly compared with the normal group (Fig. 3B). These results demonstrated that inactivated NF-κB represses the inflammatory response.

Inflammatory response is inhibited following inhibition of NF-κB

The levels of IL-6, IL-8, IL-10 and TNF-α were determined using ELISA in an attempt to investigate the effect of the TLR4/NF-κB signaling pathway on the inflammatory response. No marked difference was recorded in the level of IL-6, IL-8, IL-10 or TNF-α between the normal group, sham group and GERD + PDTC group (IL-6: $P_{Normal\ VS\ Sham} = 0.995$, $P_{Normal\ VS\ GERD+PDTC} = 0.665$, $P_{Sham\ VS\ GERD+PDTC} = 0.877$; IL-8: $P_{Normal\ VS\ Sham} = 0.981$, $P_{Normal\ VS\ GERD+PDTC} = 0.995$, $P_{Sham\ VS\ GERD+PDTC} = 0.874$; IL-10: $P_{Normal\ VS\ Sham} = 0.993$, $P_{Normal\ VS\ GERD+PDTC} = 0.211$, $P_{Sham\ VS\ GERD+PDTC} = 0.418$; TNF-α: $P_{Normal\ VS\ Sham} = 0.441$, $P_{Normal\ VS\ GERD+PDTC} = 0.292$, $P_{Sham\ VS\ GERD+PDTC} = 0.999$). The levels of the four inflammatory factors in the GERD group and GERD + LPS group were distinctly higher than those in the

normal and sham groups (IL-6: $P_{Sham\ VS\ GERD} = 0.002$; for the rest: all $P < 0.0001$). Compared with the GERD group, a significant decrease in IL-6, IL-8, IL-10 and TNF-α levels in the GERD + PDTC group (IL-6: $P_{GERD\ VS\ GERD+PDTC} = 0.033$; or the rest: all $P < 0.0001$) and an increase in the GERD + LPS group were recorded (all $P < 0.0001$) (Table 2). The obtained results indicated that decreased NF-κB allays the inflammatory response.

Table 2. The contents of IL-6, IL-8, IL-10 and TNF-α in the esophageal mucosal tissue homogenate of rats in each group (pg/mL). Notes: *, P < 0.05 vs. rats in the normal and sham groups; #, P < 0.05 vs. rats in the GERD group; GERD, gastroesophageal reflux disease; PDTC, pyrrolidine dithiocarbamate; LPS, lipopolysaccharide; IL, interleukin; TNF-α, tumor necrosis factor-alpha

Group	IL-6	IL-8	IL-10	TNF-α
Normal	136.91 ± 6.81	37.62 ± 5.37	44.41 ± 2.21	83.11 ± 1.91
Sham	138.51 ± 11.71	36.44 ± 4.56	45.01 ± 2.81	85.61 ± 2.51
GERD	154.30 ± 10.11*	48.52 ± 5.26*	73.31 ± 3.41*	113.11 ± 3.81*
PDTC	142.31 ± 9.11#	38.47 ± 6.69#	47.51 ± 3.51#	86.01 ± 5.41#
LPS	180.81 ± 10.71*#	59.53 ± 3.67*#	85.21 ± 5.01*#	134.21 ± 3.31*#

Inactivation of NF-κB contributes to decreased contents of TBARS and ROS

Here, ELISA was conducted to determine the OS-related indicators TBARS and ROS in the esophageal mucosa of rats in each group. The results shown in Table 3 suggested that in comparison to the normal group, the contents of TBARS and ROS exhibited no significant difference in the sham group (ROS: $P_{Normal\ VS\ Sham} = 0.895$, $P_{Normal\ VS\ GERD+PDTC} = 0.157$, $P_{Sham\ VS\ GERD+PDTC} = 0.625$; TBARS: $P_{Normal\ VS\ Sham} = 0.653$, $P_{Normal\ VS\ GERD+PDTC} = 0.185$, $P_{Sham\ VS\ GERD+PDTC} = 0.909$). Compared with the normal and sham groups, the GERD and GERD + LPS groups exhibited elevated contents of TBARS and ROS (all $P < 0.0001$). In comparison to the GERD group, the contents of TBARS and ROS were decreased in the GERD + PDTC group (all $P < 0.0001$) but increased in the GERD + LPS group (ROS: $P_{GERDl\ VS\ GERD+LPS} < 0.0001$; TBARS: $P_{GERD\ VS\ GERD+LPS} = 0.008$). The above findings suggested that the contents of TBARS and ROS were decreased in esophageal mucosa tissues with the inhibition of NF-κB.

Table 3. Contents of TBARS and ROS in esophageal mucosa tissues of rats in each group. Notes: *, P < 0.05, vs. the normal and sham groups; #, P < 0.05, vs. the GERD group; TBARS, thiobarbituric acid-reactive species; ROS, reactive oxygen species; GERD, gastroesophageal reflux disease; PDTC, pyrrolidine dithiocarbamate; LPS, lipopolysaccharide

Group	ROS (μmol/mg)	TBARS (μg/g)
Normal	45.21± 3.38	22.12 ± 2.36
Sham	47.42± 4.23	23.89 ± 2.79
GERD	73.57 ± 6.51*	38.98 ± 3.85*
GERD + PDTC	50.87 ± 5.01*#	25.01± 2.39*#
GERD + LPS	96.72 ± 9.13*#	43.53 ± 4.08*#

Esophageal mucosa tissues show decreased MMP-3 and MPP-9 but elevated Cldn1 and Cldn4 owing to inactivated NF-κB

Immunohistochemistry was employed to detect the expression of MMP-3, MPP-9, Cldn1, and Cldn4 in esophageal mucosa tissues, the results of which are illustrated in Fig. 4A-B, suggesting that MMP-3 and MPP-9 were predominately expressed in the cytoplasm, while Cldn1 and Cldn4 were mainly expressed in the cell membrane. In comparison to the normal group, the expression of MMP-3, MPP-9, Cldn1, and Cldn4 in the sham and GERD + PDTC groups exhibited no significant difference (MMP-3: $P_{Normal\ VS\ Sham} = 0.945$, $P_{Normal\ VS\ GERD+PDTC} = 0.603$, $P_{Sham\ VS\ GERD+PDTC} = 0.955$; MMP-9: $P_{Normal\ VS\ Sham} = 0.875$, $P_{Normal\ VS\ GERD+PDTC} = 0.189$, $P_{Sham\ VS\ GERD+PDTC} = 0.715$; Cldn1: $P_{Normal\ VS\ Sham} = 0.889$, $P_{Normal\ VS\ GERD+PDTC} = 0.301$, $P_{Sham\ VS\ GERD+PDTC} = 0.836$; Cldn4: $P_{Normal\ VS\ Sham} = 0.954$, $P_{Normal\ VS\ GERD+PDTC} = 0.649$, $P_{Sham\ VS\ GERD+PDTC} = 0.963$).

Compared with the normal and sham groups, the GERD and GERD + LPS group presented elevated MMP-3 and MPP-9 in the cytoplasm but downregulated Cldn1 and Cldn4 in the cell membrane (all $P < 0.0001$). In comparison to the GERD group, the expression of MMP-3 and MPP-9 significantly declined and that of Cldn1 and Cldn4 distinctly upregulated in esophageal mucosa tissues in the GERD + PDTC group all $P < 0.0001$); the GERD + LPS group presented increased MMP-3 and MPP-9 but decreased Cldn1 and Cldn4 (all $P < 0.0001$). Thus, these results led us to the conclusion that NF-κB inactivation results in the downregulation of MMP-3 and MPP-9 but elevates Cldn1 and Cldn4 in esophageal mucosa tissues.

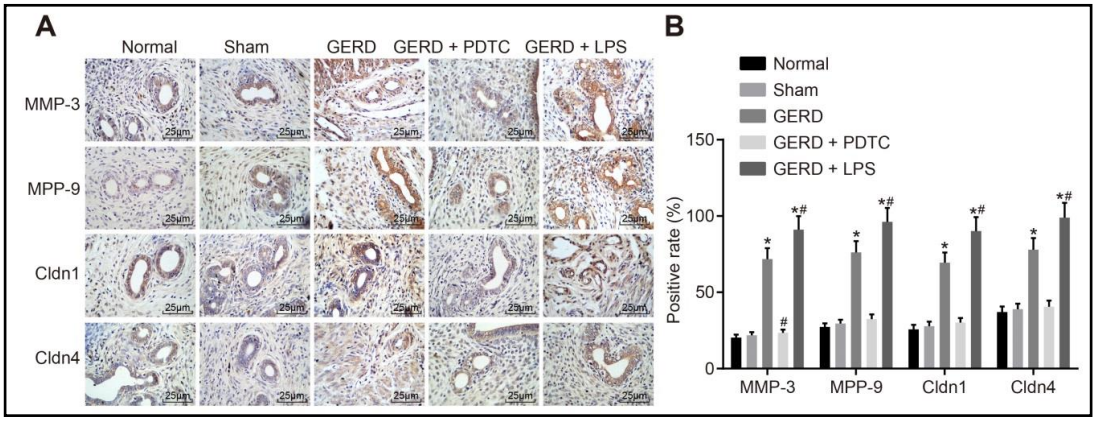

Fig. 4. Expression of MMP-3 and MPP-9 was increased, while that of Cldn1 and Cldn4 was decreased, in esophageal mucosae tissues. A, Immunohistochemistry graph of MMP-3, MPP-9, Cldn1, and Cldn4 (400 ×); B, positive expression rates of MMP-3, MPP-9, Cldn1, and Cldn4; *, P<0.05, vs. the normal and sham groups; #, P<0.05, vs. the GERD group; MMP-3, matrix metalloproteinase-3; MPP-9, matrix metalloproteinase-9; Cldn1, Claudin-1; Cldn4, Claudin-4.

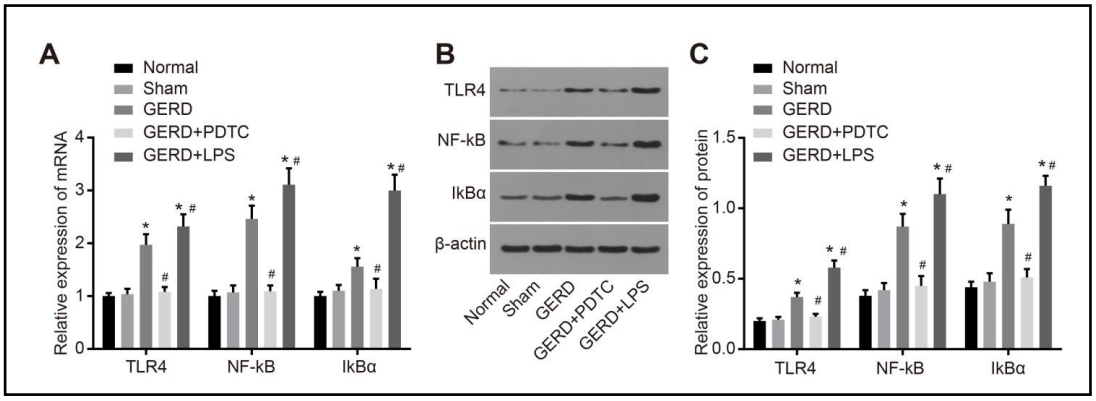

Fig. 5. Expression of the TLR4/NF-κB signaling pathway-related genes (TLR4, NF-κB and IκBα) in esophageal mucosal tissues of rats. A, mRNA expression of TLR4, NF-κB and IκBα in esophageal mucosal tissues of rats; B, protein expression of TLR4, NF-κB and IκBα in esophageal mucosal tissues; C, gray value of TLR4, NF-κB and IκBα protein bands in esophageal mucosal tissues; *, P<0.05 vs. rats in the normal group and sham group; #, P<0.05 vs. rats in the GERD group; GERD, gastroesophageal reflux disease; PDTC, pyrrolidine dithiocarbamate; LPS, lipopolysaccharide; TLR4, Toll-like receptor 4; NF-κB, nuclear factor-kappa B.

Inhibited NF-κB inactivates the TLR4/NF-κB signaling pathway

RT-qPCR and western blot analysis were applied to detect TLR4, NF-κB and IκBα mRNA and protein expressions. Compared with the normal and sham groups, the mRNA and protein expressions of TLR4, NF-κB and IκBα in the GERD + PDTC group displayed marginal increase, which were not statistically significant (mRNA: TLR4: $P_{\text{Normal VS Sham}} = 0.967$, $P_{\text{Normal VS GERD+PDTC}} = 0.696$, $P_{\text{Sham VS GERD+PDTC}} = 0.967$; NF-κB: $P_{\text{Normal VS Sham}} = 0.909$, $P_{\text{Normal VS GERD+PDTC}} = 0.801$, $P_{\text{Sham VS GERD+PDTC}} = 0.999$; IκBα: $P_{\text{Normal VS Sham}} = 0.675$, $P_{\text{Normal VS GERD+PDTC}} = 0.352$, $P_{\text{Sham VS GERD+PDTC}} = 0.984$; protein: TLR4: $P_{\text{Normal VS Sham}} = 0.927$, $P_{\text{Normal VS GERD+PDTC}} = 0.125$, $P_{\text{Sham VS GERD+PDTC}} = 0.494$; NF-κB: $P_{\text{Normal VS Sham}} = 0.703$; $P_{\text{Normal VS GERD+PDTC}} = 0.179$, $P_{\text{Sham VS GERD+PDTC}} = 0.871$; IκBα: $P_{\text{Normal VS Sham}} = 0.616$, $P_{\text{Normal VS GERD+PDTC}} = 0.108$, $P_{\text{Sham VS GERD+PDTC}} = 0.822$). In contrast, the expressions of TLR4, NF-κB and IκBα increased in the GERD and GERD + LPS groups (all $P < 0.0001$). The expressions of TLR4, NF-κB and IκBα in the GERD group were evidently lower than that of the GERD + LPS group (all $P < 0.0001$) but higher than that of the GERD + PDTC group (all $P < 0.0001$) (Fig. 5A-C). Therefore, inhibition of NF-κB inactivated the TLR4/NF-κB signaling pathway.

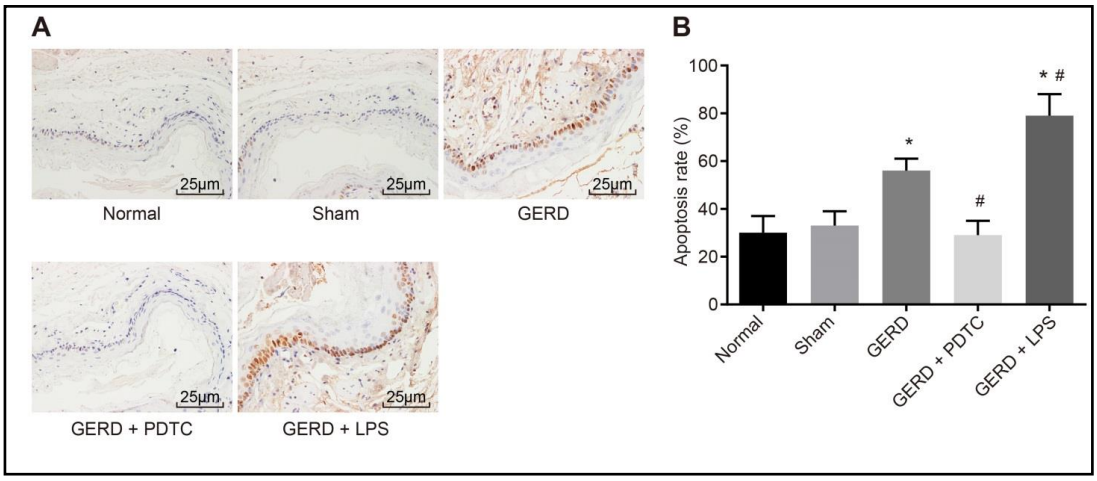

Fig. 6. Cell apoptosis in esophageal mucosal tissues of rats. A, TUNEL assay pattern of cells from the five groups (400 ×); B, apoptosis rate of the five groups; *, P<0.05 vs. rats in the normal group and sham group; #, P<0.05 vs. rats in the GERD group; GERD, gastroesophageal reflux disease; PDTC, pyrrolidine dithiocarbamate; LPS, lipopolysaccharide; TUNEL, terminal dUTP nick-end labeling.

Inactivation of NF-κB suppresses cell apoptosis in esophageal mucosal tissues

Cells containing pale-brown particles were regarded as apoptotic cells in TUNEL staining. Few apoptotic cells were detected in the normal, sham and GERD + PDTC groups under the 400 × microscope. However, in the GERD and GERD + LPS groups, a greater number of apoptotic cells was found. The apoptotic cells were subsequently counted, with the apoptotic rate calculated and compared between groups. Compared with the normal and sham groups, no significant difference in apoptotic rate was detected in the GERD + PDTC group ($P_{\text{Normal VS Sham}} = 0.811$, $P_{\text{Normal VS GERD+PDTC}} = 0.996$, $P_{\text{Sham VS GERD+PDTC}} = 0.596$), while an obvious increase was observed in that of the GERD and GERD + LPS groups ($P < 0.0001$). The apoptotic rate in the GERD group was much higher than that in the GERD + PDTC group but lower than that in the GERD + LPS group (all $P < 0.0001$) (Fig. 6A-B). The inactivation of NF-κB had an inhibitory effect on cell apoptosis in esophageal mucosal tissues.

Discussion

GERD is a common clinical disorder affecting millions of people worldwide, which results in a significant morbidity, a reduction in quality of life, and an increased cost that burdens health care systems around the world [17]. Patients with GERD often suffer from mucosal injury in the esophagus, characterized by nonspecific inflammatory infiltrate surrounding the epithelial cells that have been damaged by acid [18]. The current study set out to investigate the effect of the TLR4/NF-κB signaling pathway on esophageal mucosal injury in rats with GERD and uncovered some important findings, all of which point to the conclusion that the inhibition of the TLR4/NF-κB signaling pathway reduces the time needed to repair esophageal mucosal injury in rats with GERD.

Traditional pH parameters are competent predictive tools in GERD, with increasing acid exposure time correlated with a higher degree of esophagitis [19]. In the current study, the LPS group exhibited the lowest esophageal pH among the five groups, indicating that LPS activated the NF-κB signaling pathway, resulting in a greater degree of mucosal injuries. Key observations indicated that esophageal mucosal injuries were well-healed in the PDTC group, while symptoms of hyperemia and erosions were noted in the GERD and LPS groups. Yu Fang et al. concluded that treatment with an NF-κB inhibitor suppressed NF-κB-regulated cytokines and inhibited damage to esophageal barrier function, findings that are largely consistent with those of the present study [20]. PDTC, a potent inhibitor

of the NF-κB signal pathway, has been frequently employed to investigate the influence of NF-κB in its transcription of many target genes. For example, a previous study reported that pretreatment with PDTC could attenuate the pain behaviors of rats with diabetic neuropathy [21]. A study evaluating the relationship between TLR4 and mucosal injury demonstrated that moderate TLR4 signaling was the best for mucosal healing: insufficient TLR4 signaling caused bacterial translocation and poor mucosal healing, while too much TLR4 signaling induced severe inflammation or even cancer [22]. Another study asserted that LPS signaling could directly regulate the effect of TLR4 on Cox-2 expression as well as other downstream mediators of epithelial repair in intestinal epithelial cells [23].

Interestingly, a key observation made in the current study revealed that esophageal mucosa tissues exhibited reduced levels of MMP-3 and MPP-9 while displaying elevated Cldn1 and Cldn4 following treatment with PDTC, the inhibitor of NF-κB. The expression of NF-κB/p65 has been positively correlated with MMP-3 and MMP-9 [24]. In osteoarthritic chondrocytes, the inhibition of NF-κB has been suggested to decrease apoptosis while acting to downregulate MMP-9 [25]. Consistently, as an activator of MMP-9, MMP-3 reduction in malignant gliomas was induced by inactivated NF-κB [26]. Claudins are members of the class of proteins involved in tight junctions [27]. Cldn1 and Cldn4 expression has been detected in many cancers, including ovarian cancer and esophageal cancer [28, 29]. In line with the findings of our study, Yu et al. also demonstrated that Cldn1 and Cldn4 overexpression was induced by the inactivation of NF-κB in GERD [20].

LPS-treated rats exhibited the highest levels of IL-6, IL-8, IL-10 and TNF-α compared with other four groups. The PDTC-treated group displayed distinct inflammatory factor level reductions. Several studies have investigated the association between gene expression and inflammation, for example, inflammation in claudin-7-deficient mice, NOD-Like receptor protein 3 inflammasome priming and 5-HT4 receptor agonist mosapride in inflammation of reflux esophagitis [30-32]. Inflammation is a useful host response to tissue injury that aids in tissue regeneration, facilitating the return to normal function and structure. This being said, prolonged inflammation leads to serious tissue damage; LPS upregulates TLR4, leading to NF-κB activation, and consequently prolongs the inflammatory response [33]. NF-κB positively regulates the levels of IL-1β, IL-6, and IL-8 in immune and epithelial cells, which in turn by direct or indirect means activates NF-κB via signaling pathways [34]. Investigations of the inflammatory mediator profile in GERD presented evidence indicating increased activity of NF-κB in the mucosa of GERD patients demonstrating that the inflammatory response is correlated with proinflammatory cytokine levels, such as L-1, IL-6, and IL-8, in the esophageal mucosa [18].

During the current study, we demonstrated that GERD rats administered LPS treatment displayed elevated mRNA and protein expression of TLR4/NF-κB signaling pathway components, and increased apoptosis rate; when treated with the NF-κB pathway inhibitor PDTC, the GERD rats presented reduced mRNA and protein expression of TLR4/NF-κB signaling pathway components Consistently, mRNA and protein levels of TLR4 have been observed to be significantly increased with the treatment of LPS [35]. A reduction in expression levels of TLR4 and NF-κB is an efficient way for carvedilol to inhibit ischemia/reperfusion-induced apoptosis [36]. Taking all of our findings and previous findings together, we speculate that TLR4 activates the transcription of inflammation cytokines as well as pro-apoptotic signaling that results in cell death. TLR4 activated by LPS triggers the downstream apoptotic signaling pathways and modulates the expression of Bax, Bcl-2, and caspase-3 [35].

Conclusion

In conclusion, GERD-induced esophageal mucosal injury could potentially be repaired through inhibition of the TLR4/NF-κB signaling pathway, highlighting the TLR4/NF-κB pathway as a promising potential therapeutic target for GERD. Further studies are needed to validate the findings of our study.

Acknowledgements

We thank the reviewers for critical comments.

Disclosure Statement

The authors declare no conflicts of interest.

References

1 Liu BY, Lin YJ, Lee HF, Ho CY, Ruan T, Kou YR: Menthol suppresses laryngeal C-fiber hypersensitivity to cigarette smoke in a rat model of gastroesophageal reflux disease: the role of TRPM8. J Appl Physiol (1985) 2015;118:635-645.
2 Mohammadi M, Ramezani Jolfaie N, Alipour R, Zarrati M: Is Metabolic Syndrome Considered to Be a Risk Factor for Gastroesophageal Reflux Disease (Non-Erosive or Erosive Esophagitis)?: A Systematic Review of the Evidence. Iran Red Crescent Med J 2016;18:e30363.
3 El-Serag HB, Sweet S, Winchester CC, Dent J: Update on the epidemiology of gastro-oesophageal reflux disease: a systematic review. Gut 2014;63:871-880.
4 Lin HC, Xirasagar S, Chung SD, Huang CC, Tsai MC, Chen CH: Fewer acute respiratory infection episodes among patients receiving treatment for gastroesophageal reflux disease. PLoS One 2017;12:e0172436.
5 Nwokediuko SC: Current trends in the management of gastroesophageal reflux disease: a review. ISRN Gastroenterol 2012;2012:391631.
6 Mahadeva S, Raman MC, Ford AC, Follows M, Axon AT, Goh KL, Moayyedi P: Gastro-oesophageal reflux is more prevalent in Western dyspeptics: a prospective comparison of British and South-East Asian patients with dyspepsia. Aliment Pharmacol Ther 2005;21:1483-1490.
7 Triantos C, Koukias N, Karamanolis G, Thomopoulos K: Changes in the esophageal mucosa of patients with non erosive reflux disease: How far have we gone? World J Gastroenterol 2015;21:5762-5767.
8 Choo BK, Roh SS: Berberine protects against esophageal mucosal damage in reflux esophagitis by suppressing proinflammatory cytokines. Exp Ther Med 2013;6:663-670.
9 Taddei A, Fabbroni V, Pini A, Lucarini L, Ringressi MN, Fantappie O, Bani D, Messerini L, Masini E, Bechi P: Cyclooxygenase-2 and inflammation mediators have a crucial role in reflux-related esophageal histological changes and Barrett's esophagus. Dig Dis Sci 2014;59:949-957.
10 Brzozowska I, Strzalka M, Drozdowicz D, Konturek SJ, Brzozowski T: Mechanisms of esophageal protection, gastroprotection and ulcer healing by melatonin. implications for the therapeutic use of melatonin in gastroesophageal reflux disease (GERD) and peptic ulcer disease. Curr Pharm Des 2014;20:4807-4815.
11 Xiang NL, Liu J, Liao YJ, Huang YW, Wu Z, Bai ZQ, Lin X, Zhang JH: Abrogating ClC-3 Inhibits LPS-induced Inflammation via Blocking the TLR4/NF-kappaB Pathway. Sci Rep 2016;6:27583.
12 Feng Y, Cui Y, Gao JL, Li MH, Li R, Jiang XH, Tian YX, Wang KJ, Cui CM, Cui JZ: Resveratrol attenuates neuronal autophagy and inflammatory injury by inhibiting the TLR4/NF-kappaB signaling pathway in experimental traumatic brain injury. Int J Mol Med 2016;37:921-930.
13 Wang Y, Mao L, Zhang L, Zhang L, Yang M, Zhang Z, Li D, Fan C, Sun B: Adoptive Regulatory T-cell Therapy Attenuates Subarachnoid Hemor-rhage-induced Cerebral Inflammation by Suppressing TLR4/NF-B Signaling Pathway. Curr Neurovasc Res 2016;13:121-126.
14 Zhang QQ, Ding Y, Lei Y, Qi CL, He XD, Lan T, Li JC, Gong P, Yang X, Geng JG, Wang LJ: Andrographolide suppress tumor growth by inhibiting TLR4/NF-kappaB signaling activation in insulinoma. Int J Biol Sci 2014;10:404-414.
15 Xu XM, Ning YC, Wang WJ, Liu JQ, Bai XY, Sun XF, Cai GY, Chen XM: Anti-Inflamm-Aging Effects of Long-Term Caloric Restriction via Overexpression of SIGIRR to Inhibit NF-kappaB Signaling Pathway. Cell Physiol Biochem 2015;37:1257-1270.
16 Ganz RA: A Modern Magnetic Implant for Gastroesophageal Reflux Disease. Clin Gastroenterol Hepatol 2017;15:1326-1337.

17 Bor S, Kitapcioglu G, Kasap E: Prevalence of gastroesophageal reflux disease in a country with a high occurrence of Helicobacter pylori. World J Gastroenterol 2017;23:525-532.
18 Rieder F, Biancani P, Harnett K, Yerian L, Falk GW: Inflammatory mediators in gastroesophageal reflux disease: impact on esophageal motility, fibrosis, and carcinogenesis. Am J Physiol Gastrointest Liver Physiol 2010;298:G571-581.
19 Patel A, Sayuk GS, Gyawali CP: Parameters on esophageal pH-impedance monitoring that predict outcomes of patients with gastroesophageal reflux disease. Clin Gastroenterol Hepatol 2015;13:884-891.
20 Fang Y, Chen H, Hu Y, Djukic Z, Tevebaugh W, Shaheen NJ, Orlando RC, Hu J, Chen X: Gastroesophageal reflux activates the NF-kappaB pathway and impairs esophageal barrier function in mice. Am J Physiol Gastrointest Liver Physiol 2013;305:G58-65.
21 Huang Y, Zang Y, Zhou L, Gui W, Liu X, Zhong Y: The role of TNF-alpha/NF-kappa B pathway on the up-regulation of voltage-gated sodium channel Nav1.7 in DRG neurons of rats with diabetic neuropathy. Neurochem Int 2014;75:112-119.
22 Fukata M, Shang L, Santaolalla R, Sotolongo J, Pastorini C, Espana C, Ungaro R, Harpaz N, Cooper HS, Elson G, Kosco-Vilbois M, Zaias J, Perez MT, Mayer L, Vamadevan AS, Lira SA, Abreu MT: Constitutive activation of epithelial TLR4 augments inflammatory responses to mucosal injury and drives colitis-associated tumorigenesis. Inflamm Bowel Dis 2011;17:1464-1473.
23 Fukata M, Chen A, Klepper A, Krishnareddy S, Vamadevan AS, Thomas LS, Xu R, Inoue H, Arditi M, Dannenberg AJ, Abreu MT: Cox-2 is regulated by Toll-like receptor-4 (TLR4) signaling: Role in proliferation and apoptosis in the intestine. Gastroenterology 2006;131:862-877.
24 Hu X, Tang J, Pan J, Wu G: [Study of the expression of nuclear factor-kappa B, matrix metalloproteinase-3, -9 on nasopharyngeal carcinoma and their clinical significance]. Lin Chung Er Bi Yan Hou Tou Jing Wai Ke Za Zhi 2010;24:678-682.
25 Wang Y, Li de L, Zhang XB, Duan YH, Wu ZH, Hao DS, Chen BS, Qiu GX: Increase of TNFalpha-stimulated osteoarthritic chondrocytes apoptosis and decrease of matrix metalloproteinases 9 by NF-kappaB inhibition. Biomed Environ Sci 2013;26:277-283.
26 Sun P, Mu Y, Zhang S: A novel NF-kappaB/MMP-3 signal pathway involves in the aggressivity of glioma promoted by Bmi-1. Tumour Biol 2014;35:12721-12727.
27 Overgaard CE, Daugherty BL, Mitchell LA, Koval M: Claudins: control of barrier function and regulation in response to oxidant stress. Antioxid Redox Signal 2011;15:1179-1193.
28 Jeong HM, Kwon MJ, Shin YK: Overexpression of Cancer-Associated Genes via Epigenetic Derepression Mechanisms in Gynecologic Cancer. Front Oncol 2014;4:12.
29 Takala H, Saarnio J, Wiik H, Soini Y: Claudins 1, 3, 4, 5 and 7 in esophageal cancer: loss of claudin 3 and 4 expression is associated with metastatic behavior. APMIS 2007;115:838-847.
30 Ding L, Lu Z, Foreman O, Tatum R, Lu Q, Renegar R, Cao J, Chen YH: Inflammation and disruption of the mucosal architecture in claudin-7-deficient mice. Gastroenterology 2012;142:305-315.
31 Nadatani Y, Huo X, Zhang X, Yu C, Cheng E, Zhang Q, Dunbar KB, Theiss A, Pham TH, Wang DH, Watanabe T, Fujiwara Y, Arakawa T, Spechler SJ, Souza RF: NOD-Like Receptor Protein 3 Inflammasome Priming and Activation in Barrett's Epithelial Cells. Cell Mol Gastroenterol Hepatol 2016;2:439-453.
32 Zhuang ZH, Zou FM, Tang DP, Zhuang JY, Wei JJ, Yang LY: The 5-HT4 receptor agonist mosapride attenuates inflammation of reflux esophagitis. Hepatogastroenterology 2014;61:115-119.
33 Liu L, Li YH, Niu YB, Sun Y, Guo ZJ, Li Q, Li C, Feng J, Cao SS, Mei QB: An apple oligogalactan prevents against inflammation and carcinogenesis by targeting LPS/TLR4/NF-kappaB pathway in a mouse model of colitis-associated colon cancer. Carcinogenesis 2010;31:1822-1832.
34 Korkaya H, Liu S, Wicha MS: Regulation of cancer stem cells by cytokine networks: attacking cancer's inflammatory roots. Clin Cancer Res 2011;17:6125-6129.
35 Song X, Guo M, Wang T, Wang W, Cao Y, Zhang N: Geniposide inhibited lipopolysaccharide-induced apoptosis by modulating TLR4 and apoptosis-related factors in mouse mammary glands. Life Sci 2014;119:9-17.
36 Zhao Y, Xu Y, Zhang J, Ji T: Cardioprotective effect of carvedilol: inhibition of apoptosis in H9c2 cardiomyocytes via the TLR4/NF-kappaB pathway following ischemia/reperfusion injury. Exp Ther Med 2014;8:1092-1096.